ACS APPLIED MATERIALS & INTERFACES

Research Article

www.acsami.org

Synergistic Effect on Corrosion Resistance of Phynox Substrates Grafted with Surface-Initiated ATRP (Co)polymerization of 2-Methacryloyloxyethyl Phosphorylcholine (MPC) and 2-Hydroxyethyl Methacrylate (HEMA)

Bastien Barthélémy,[†] Simon Maheux,[†] Sébastien Devillers,[†] Frédéric Kanoufi,[‡] Catherine Combellas,[‡] Joseph Delhalle,[†] and Zineb Mekhalif*[,†]

[†]Laboratory of Chemistry and Electrochemistry of Surfaces (CES) University of Namur, 61 Rue de Bruxelles, B-5000 Namur, Belgium

[‡]Laboratoire Interfaces Traitements Organisation et Dynamique des Système (ITODYS), Université Paris Diderot, CNRS UMR 7086, 15 Rue Jean Antoine de Baïf, F-75013 Paris, France

Supporting Information

ABSTRACT: Phynox is of high interest for biomedical applications due to its biocompatibility and corrosion resistance. However, some Phynox applications require specific surface properties. These can be imparted with suitable surface functionalizations of its oxide layer. The present work investigates the surface-initiated atom transfer radical polymerization (ATRP) of 2-methacryloyoxyethyl phosphorylcholine (MPC), 2-hydroxyethyl methacrylate (HEMA), and ATRP copolymerization of (HEMA-*co*-MPC) (block and statistic copolymerization with different molar ratios) on grafted Phynox substrates modified with 11-(2-bromoisobutyrate)-undecyl-1-phosphonic acid (BUPA) as initiator. It is found that ATRP (co)-polymerization of these monomers is feasible and forms hydrophilic layers, while improving the corrosion resistance of the system.

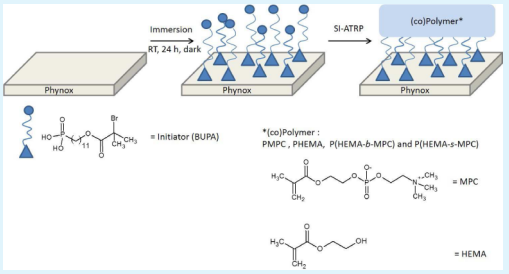

KEYWORDS: *Phynox, 11-(2-bromoisobutyrate)-undecyl-1-phosphonic acid, surface modification, surface-initiated ATRP, 2-methacryloyloxyethyl phosphorylcholine, 2-hydroxyethyl methacrylate*

1. INTRODUCTION

Phynox is an austenitic cobalt−chromium alloy (AFNOR designation K13C20N16Fe15D07) exhibiting a variety of chemical, physical, and biochemical properties such as resistance to corrosion and high passivity in contact with human tissues.[1,2] Due to these properties, Phynox is used in many biomedical applications (medical instruments, stents, pacemaker electrodes, implants, ...).[3−5] However, evaluation of explanted stents after in vivo implantation reveals electrochemical and mechanically induced corrosions.[6] Hence, modifications of the surface Phynox oxide layer to enhance resistance to electrochemical corrosion and simultaneously conferring suitable properties (antifouling, reduction of protein adsorption, ...) for biomedical applications are highly desirable. Different physical techniques such as plasma based surface modification, laser implantation, ion beam and physical vapor deposition are commonly used for surface modification.[7] Chemical techniques such as electropolymerization, polymerization, and chemical vapor deposition are also reported in that context.[7]

A more versatile approach, which is gaining increasing importance, is to build strongly adherent thin films and/or polymer layers on the surfaces of interest. For example, Ishihara et al. have much contributed to the development of surface-initiated atom transfer radical polymerization (SI-ATRP) of different monomers such as HEMA and MPC to form hydrophilic and biocompatible layers.[8] ATRP has become a powerful technique for the preparation of valuable multifunctional materials in biology and medicine.[8] Moreover, it is a method of choice because it allows control of the chain length, thickness, composition of the polymer brushes and is appropriate for the synthesis of well-defined copolymers.[9] In their work Ishihara et al. mainly considered Si and SiO_2 substrates modified with organosilanes based ATRP initiators. However, silane derivatives grafted on metal oxide surfaces are comparatively more sensitive to hydrolysis[10,11] in physiological pH conditions than their organophosphonic acid analogues. Due to their remarkable resistance to homocondensation[12,13] and ability to bind strongly on a large variety of metal oxide surfaces (including the most commonly used alloys in the biomaterials field, that is, SS316L,[14] Nitinol,[15−17] and Phynox[1,18,19]) organophosphonic acids are candidates of choice

Received: February 3, 2014
Accepted: June 10, 2014
Published: June 10, 2014

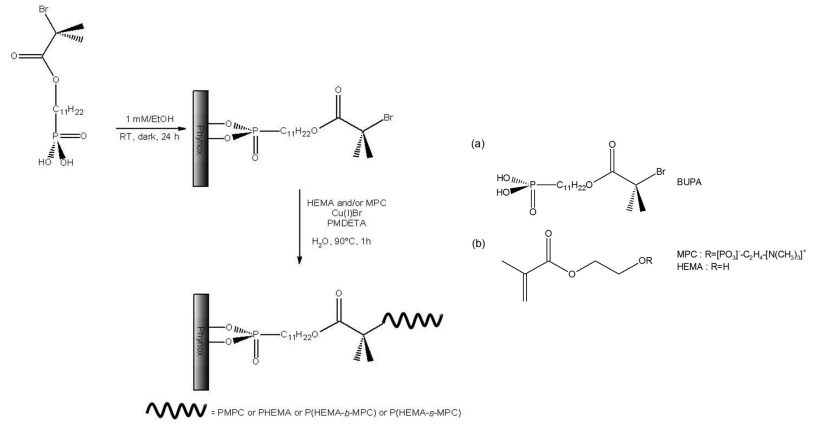

Figure 1. Schematic of the Phynox surface modification methodology used in this work and chemical structure of 11-(2-bromoisobutyrate)-undecyl-1-phosphonic acid (BUPA) (a), 2-(methacryloyloxy)ethyl 2-(trimethylammonio)ethyl phosphate (MPC) and 2-hydroxyethyl methacrylate (HEMA) (b).

as anchoring groups for the elaboration of corrosion resistant SI-ATRP platforms. Babu et al. have reported the synthesis of 2-bromo-2-methyl-propionic acid 2-phosphonooxy-ethyl ester, and its grafting on magnetite nanoparticles of polymer brushes (PMMA and PS) by ATRP.[20,21] Kim et al. have formed ferrocene functional polymer brushes on ITO using 6-(2-bromo-2-methylpropanoyloxo)hexylphosphonic acid as SI-ATRP initiator.[22] In our group, stainless steel (AISI304) has been modified with 11-(2-bromoisobutyrate)-undecyl-1-phosphonic acid (BUPA) to form PMMA, PS and diblock PS-*b*-PMMA brushes by SI-ATRP.[23] More recently, we have succeeded in forming MPC polymer brushes on Nitinol[16] and Phynox[19] with the BUPA initiator.

The aim of the present work is to modify Phynox surfaces with a BUPA monolayer (Figure 1) on which MPC and HEMA were subsequently polymerized. PMPC is well-known for its hydrophilic character and ability to avoid protein adsorption and cell adhesion.[24−27] PHEMA is also known to be hydrophilic and hemocompatible.[27,28] All these properties are essential in the frame of biomedical applications such as cardiovascular implants, surgical tools, etc. Ishihara et al. showed that the thickness of PMPC and PHEMA layers is important both for the wettability and the reduction of protein adsorptions on the coated substrates.[29] Hence, the formation by SI-ATRP substrates of HEMA and MPC copolymers, diblock or statistical, on modified Phynox is the core contribution of this work. ATRP constitutes the most simple and efficient way to generate such multilayered structure. Indeed, owing to its living character, the ATRP polymerization process generates dormant polymeric chains that can be further activated in subsequent ATRP baths. Since HEMA is much cheaper than MPC, it is economically interesting to form a first hydrophilic and hemocompatible PHEMA layer on which a thinner PMPC layer is then formed by block copolymerization, P(HEMA-*b*-MPC), in order to impart resistance to protein adsorption and cell adhesion to the surface. However, statistic copolymerization, P(HEMA-*s*-MPC), has the principal advantage of an easier experimental modus operandi. It is, therefore, interesting to compare the properties of P(HEMA-*s*-MPC) with those of P(HEMA-*b*-MPC). The different steps of this work are schematically described in Figure 1.

2. MATERIALS AND METHODS

2.1. Chemicals. Phynox substrates (foils of about 0.1 mm thickness) were purchased from Arcelor Mittal Imphy Service, Clichy, France. This alloy is mainly composed of Co (39−41%), Cr (19−21%), Ni (15−16%), Mo (6.5−7.5%), Mn (1.5−2.0%), and Fe (balance) with small percentages of other elements such as Si (≤1.2%), C (≤0.15%), P (≤0.015%), S (≤0.015%), and Be (≤0.001%). The surface composition of mechanically polished Phynox is somewhat different from the bulk composition: the main metallic elements constitutive of the outer layer assessed by XPS are Co (17%), Cr (34%), Si (17%), Fe (12%), Mn (5%), Mo (7%), and Ni (7%) after polishing (see section 2.3. for polishing details).

All reagents used for the synthesis of the BUPA were purchased from Aldrich Chemical Co.: 10-bromo-1-undecanol (98%), 3,4-dihydro-2H-pyrane (97%), *p*-toluenesulfonic acid (98%), triethyl phosphate (98%), pyridinium-*p*-toluene-sulfonate (98%), 2-bromoisobutyryl-bromide (98%), pyridine (97%) dried on CaH_2, bromotrimethylsilane (97%), anhydrous anisole (99.7%), dichloromethane, petroleum ether, diethyl ether, ethyl acetate, methanol, acetonitrile, acetone, ethanol, absolute ethanol (>99.8%), and anhydrous tetrahydrofuran. All these chemicals were used without any further purification.

Reagents for the polymerization were also purchased from Aldrich Chemical Co. and purified before use: copper(I) bromide (98%) was purified according to the method described by Keller and Wycoff.[30] *N*,*N*,*N*,*N*,*N*-pentamethyldiethylenetriamine (PMDETA, 99%) was distilled before use. 2-(methacryloyloxy)ethyl 2-(trimethylammonio)ethyl phosphate (MPC, > 96.0%) was purchased from TCI Europe and 2-hydroxyethyl methacrylate (HEMA, 97%) from Pfaltz and Bauer. Tetrahydrofuran (THF, 99%) was purchased from VWR. Sodium chloride (99.5%) and sodium hydroxide (97+%) from Acros Organics. Milli-Q water (18.2 MΩ.cm) was used for the preparation of all aqueous solutions.

2.2. Synthesis of 11-(2-Bromoisobutyrate)-undecyl-1-phosphonic Acid (BUPA). Synthesis of BUPA has been reported previously.[23] The same conditions were used in this work to form this molecule with an overall yield of 30%.

2.3. Grafting of the Initiator on the Phynox Substrates. Phynox substrates used in this work were rectangular-shaped (1 × 2 cm^2) coupons. They were mechanically mirror polished down to 1 μm using grit silicon carbide papers (SiC-paper, grit 800 and 1200 from Struers) and

water-based diamond suspensions (successively 9, 3, and 1 μm from Buehler). The polishing was carried out on a Buehler Phoenix 4000 instrument. At the end of the polishing steps, the metal coupons were cleaned by sonication 15 min in ethanol (using a Branson 1520 device with a power output of 70 W at a frequency of 42 kHz) and blown dry under a nitrogen flow. Just before modification, the substrates were cleaned again by sonication during 15 min in ethanol, blown dry under a nitrogen flow and subjected to a UV/O_3 treatment for 30 min (in a UVC-Cleaner device model No. 42-220).

The BUPA monolayer was then formed by immersing the samples in a 1 mM BUPA solution in absolute ethanol during 24 h at room temperature in the dark. They were then rinsed copiously with ethanol, cleaned by sonication 15 min in the same solvent, blown dry under a nitrogen flow, and directly characterized.

2.4. ATRP Polymerizations. *2.4.1. PMPC Films.* ATRP was carried out according to the following procedure: 10 mL of milli-Q water, 52 mg (30 mM) of PMDETA, and 0.50 g (0.17 M) of MPC were added to a reaction flask sealed with a rubber septum. The reaction mixture was deaerated five times by freeze-pump-backfilling with argon. 43 mg (30 mM) of Cu(I) Br was added to the mixture. Then, the modified substrates with BUPA were immersed in the mixture. The polymerization was allowed to proceed during 1 h at 90 °C. After the polymerization, the coated substrates were cleaned by sonication 15 min in methanol and 5 min in THF. Finally, the substrates were rinsed copiously with methanol in order to remove the untethered polymer and blown dry under a nitrogen flow.

2.4.2. PHEMA Films. ATRP was carried out following the same procedure as for PMPC except that 0.22 g (0.17 M) of HEMA was used instead of 0.50 g (0.17 M) in the case of MPC in the reaction flask.

2.4.3. P(HEMA-b-MPC) Films. Block copolymerization was performed according to the same procedure used for homopolymers in two successive steps (with 1 h of polymerization time in each step): after HEMA polymerization, substrates were copiously rinsed with milli-Q water and cleaned by sonication 15 min in methanol and 5 min in THF. The substrates were then rinsed copiously with methanol in order to remove the untethered polymer and blown dry under a nitrogen flow. The modified substrates were then immersed in a new bath for MPC polymerization. P(HEMA-*b*-MPC) were synthesized with different HEMA/MPC molar ratios of 1/1 (0.22 and 0.50 g, respectively), 2/1 (0.22 and 0.25 g, respectively), and 4/1 (0.22 and 0.12 g, respectively). After block copolymerization, the resulting substrates were copiously rinsed with milli-Q water and cleaned by sonication 15 min in methanol and 5 min in THF. Finally, the substrates were rinsed copiously with methanol in order to remove the untethered polymer and blown dry under a nitrogen flow.

2.4.4. P(HEMA-s-MPC) Films. Statistic copolymerization was performed according to the following procedure: 10 mL of milli-Q water, 52 mg (30 mM) of PMDETA, MPC, and HEMA are added to a reaction flask sealed with a rubber septum. Different HEMA/MPC molar ratios were used: 1/1 (0.22 and 0.50 g, respectively), 2/1 (0.22 and 0.25 g, respectively), and 4/1 (0.22 and 0.12 g, respectively). The reaction mixture was deaerated five times by freeze-pump-backfilling with argon. Cu(I)Br (43 mg; 30 mM) was added to the mixture. Then, the modified substrates with BUPA were immersed in the mixture. The polymerization was allowed to proceed during 1 h at 90 °C. After the statistic copolymerization, the coated substrates were cleaned by sonication 15 min in methanol and 5 min in THF. Finally, the substrates were rinsed copiously with methanol in order to remove the untethered polymer and blown dry under a nitrogen flow.

2.5. Substrates Characterizations. The modified substrates were characterized by X-ray photoelectron spectroscopy (XPS), polarization modulation infrared reflection adsorption spectroscopy (PM-IRRAS), ellipsometry, cyclic voltammetry (CV), and linear sweep voltammetry (LSV).

XPS was used to study the elemental composition of the modified substrates. The spectra have been recorded with a SSX-100 spectrometer using a monochromatized X-ray Al Kα radiation (1486.6 eV), the photoemitted electrons being collected at 35° takeoff angle relative to the surface normal. Nominal resolution was measured as full width at half-maximum of 1.0−1.5 eV for core levels and survey spectra, respectively. The binding energy of core levels was calibrated against the C 1s binding energy set at 285.0 eV, an energy characteristic of alkyl moieties. The peaks were analyzed using a combination Gaussian−Lorentzian curves (80% of Gaussian character).

PM-IRRAS data were collected from a Bruker Equinox55 PMA37 equipped with a liquid-nitrogen-cooled mercury−cadmium−telluride (MCT) detector and a zinc−selenide photoelastic modulator. The measurements were carried out with the photoelastic modulator set at half-wave retardation of 2600 cm^{-1}. The infrared light, reaching the sample surface at an angle of 80° relative to the surface normal, was modulated between s- and p-polarization at a frequency of 50 kHz. Signals generated from each polarization (Rs and Rp) were detected simultaneously by a lock-in amplifier and used to calculate the differential surface reflectivity $(\Delta R/R) = (Rp - Rs)/(Rp + Rs)$. The spectra were taken by collecting 512 scans at a spectral resolution of 2 cm^{-1}.

Static water contact angle (θ_w) measurements were carried out using a DIGIDROP (GBX Surface Science Technology) contact angle goniometer at room temperature and ambient atmosphere. A syringe was used to deliver 2.0 μL of probe droplets of milli-Q water to the sample surface.

The thickness of the formed monolayers and polymer layers has been determined by ellipsometry. Measurements have been performed on a SENTECH SE400adv ellipsometer with a He−Ne laser and an angle of incidence of 70° at a wavelength of 632.8 nm. The ellipsometer is controlled with the SE 400 Advanced 2.20 software. The refractive index n and dispersion coefficient k (imaginary part of the complex refractive index) for the Phynox substrate were obtained from the clean bare surface (2.33 and 4.13, respectively). The refractive index n of the monolayer was set at 1.45 and 1.49 for the grafted polymer layers (PMPC, PHEMA, and copolymers). The choice of these values is based on a work of Ishihara et al.[29] in which a similar initiator is used for SI-ATRP polymerization of MPC and HEMA (additional informations are available in the Supporting Informations part).

Electrochemical measurements provide additional informations on the resistance to oxidation and corrosion of Phynox imparted by the coatings elaborated in this work. Experiments were carried out with an EG&G Instruments potentiostat, model 263A, monitored by computer and M270 electrochemistry software. A three-electrode electrochemical cell was used with a standard calomel electrode (SCE) as reference electrode and a platinum foil as counter electrode. The cell

Table 1. Water Static Contact Angles of Milli-Q water (θ_w) Droplets; Ellipsometric Thickness Determination of a Bare Polished Phynox Substrate, Phynox Substrate Modified with BUPA, Modified Phynox Substrates after ATRP (Co)polymerization of MPC, HEMA, HEMA-*b*-MPC, or HEMA-*s*-MPC (with Different Molar Ratios) and Relative Abundance Ratios Calculated on the Basis of XPS Analyses and Graft Density σ of Monomer Entities (σ_{HEMA} and σ_{MPC}) for Modified Phynox Substrates after ATRP Copolymerization of $(HEMA)_n$-*b*-$(MPC)_m$ and $(HEMA)_n$-*s*-$(MPC)_m$ (with Different Molar Ratios)

substrates	θ_w (deg) ± 1°	h (nm) ± 0.2 nm	P/N	N/C_{COOR}	n/m	σ_{HEMA} (mol·cm^{-2})	σ_{MPC} (mol·cm^{-2})
bare phynox	52						
Phynox–BUPA	87	1.4					
Phynox–BUPA–PMPC	32	6.1	1.1	0.83			2.7×10^{-9}
Phynox–BUPA–PHEMA	35	23.1				2.0×10^{-8}	
Phynox–BUPA–P(HEMA-*b*-MPC) 1/1	49	26.2	1.0	0.17	4.9	2.0×10^{-8}	1.4×10^{-9}
Phynox–BUPA–P(HEMA-*b*-MPC) 2/1	47	26.7	0.9	0.17	4.9	2.0×10^{-8}	1.5×10^{-9}
Phynox–BUPA–P(HEMA-*b*-MPC) 4/1	48	26.0	1.0	0.17	5.0	2.0×10^{-8}	1.3×10^{-9}
Phynox–BUPA–P(HEMA-*s*-MPC) 1/1	49	28.5	1.1	0.07(5)	12.2	2.3×10^{-8}	1.8×10^{-9}
Phynox–BUPA–P(HEMA-*s*-MPC) 2/1	48	28.9	0.9	0.06(9)	13.5	2.4×10^{-8}	1.6×10^{-9}
Phynox–BUPA–P(HEMA-*s*-MPC) 4/1	47	28.7	1.0	0.06(3)	14.8	2.4×10^{-8}	1.5×10^{-9}

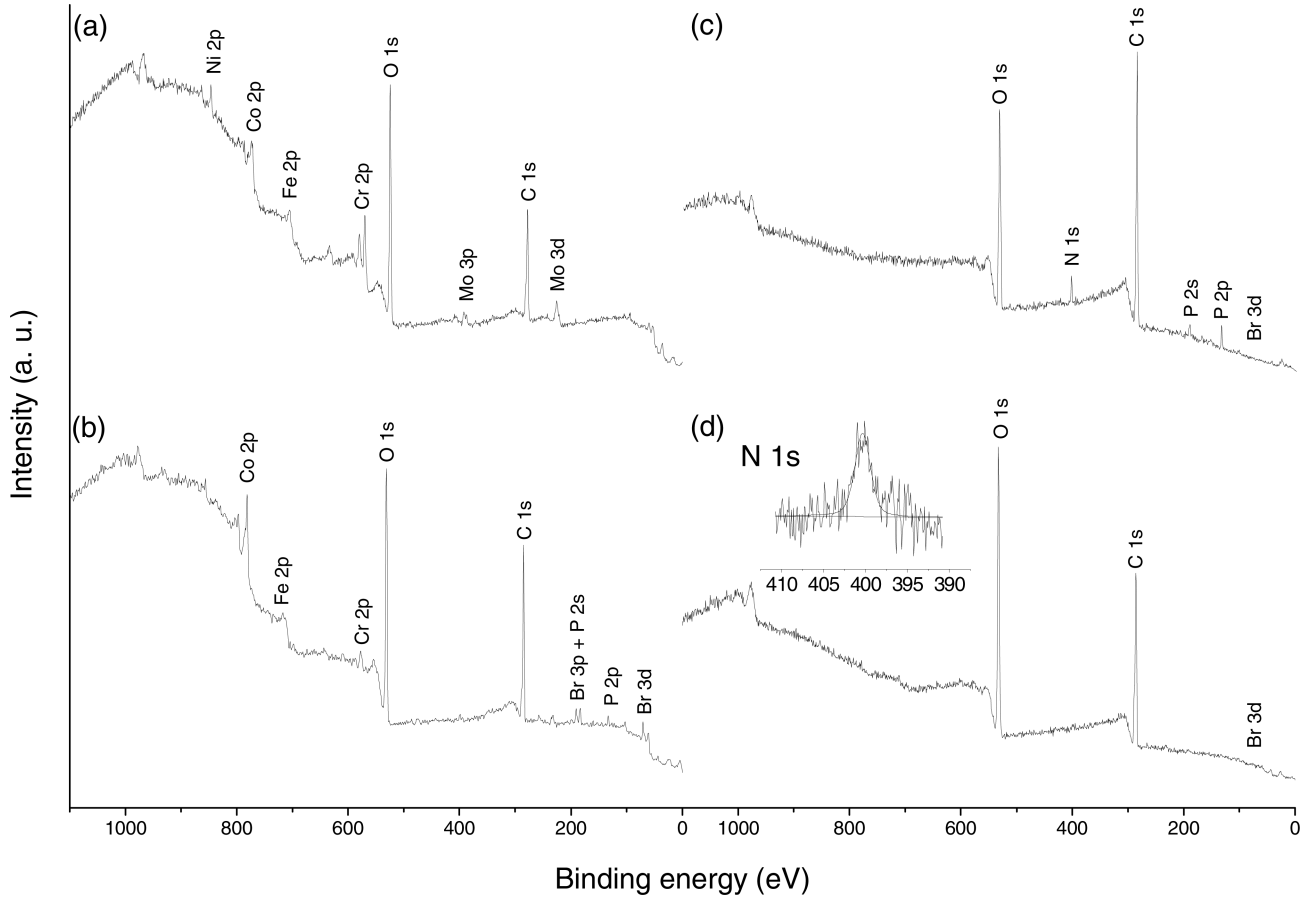

Figure 2. XPS general survey spectra of bare polished Phynox substrate (a), Phynox substrate modified with 11-(2-bromoisobutyrate)-undecyl-1-phosphonic acid (b), modified Phynox substrates after ATRP polymerization of MPC (c), or HEMA (with N 1s core level peak as an inset) (d).

used enables analysis of a well-defined and reproducible spot (0.28 cm^2) on the sample. Polarization curves experiments were carried out in a 0.5 M sodium chloride solution by sweeping the potential from −1 to +1 V at 1 mV·s^{-1}. Cyclic voltammetry experiments were performed in a 0.1 M sodium hydroxide solution by sweeping the potential from −0.6 to 0.6 V at 20 mV·s^{-1}.

For reproducibility considerations, each substrates modification and characterization has been carried out at least three times for each surface modification. Substrates have been characterized directly after modification.

3. RESULTS AND DISCUSSION

3.1. Grafting of 11-(2-Bromoisobutyrate)-undecyl-1-phosphonic Acid (BUPA) on Phynox Substrates. The grafting of BUPA (Figure 1) on Phynox has been already reported previously.[19] To ascertain reproducibility characterizations have been performed once more. The results obtained in the frame of the present work are essentially identical to those previously obtained: grafting leads to an increase of the water contact angle from 51° for a bare Phynox substrate to 87° for a modified one (Table 1). XPS analysis reveals the presence of P 2s, P 2p, Br 3p, and Br 3d core level photoelectron peaks

(characteristics of the grafted molecule) on modified substrates spectra while they are not present on the bare substrates spectra (Figure 2). Additional characterizations such as ellipsometry, linear sweep voltammetry, and cyclic voltammetry are discussed in the sequel.

Ellipsometry results are summarized in Table 1. The formed BUPA films have thicknesses of the order of 1.4 ± 0.2 nm, which is slightly smaller than the theoretical value (1.6 nm) of fully extended BUPA molecules in a dry state estimated from standard bond lengths and angles. This suggests that BUPA molecules do not form fully organized monolayers on the Phynox surface.

Linear sweep voltammetry and cyclic voltammetry results are presented in Figures 3 and 4, respectively. The grafting of

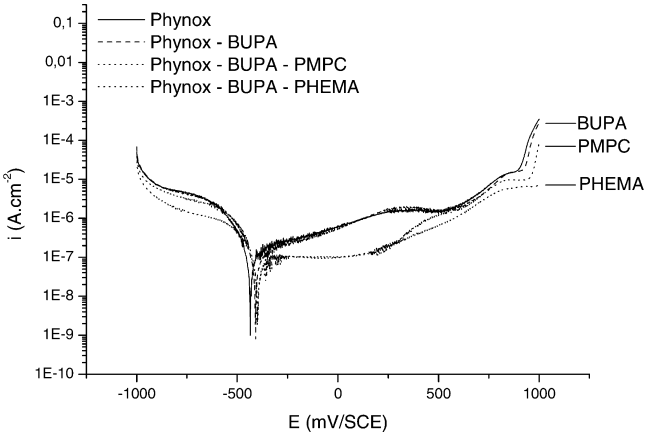

Figure 3. Linear sweep voltammetry curves of a bare polished Phynox substrate, Phynox substrate modified with 11-(2-bromoisobutyrate)-undecyl-1-phosphonic acid (BUPA), modified Phynox substrate after ATRP polymerization of MPC or HEMA. (Curves acquired by scanning potentials from −1 V/ECS to 1 V/SCE at 1 mV·s^{-1} in NaCl 0.5 M).

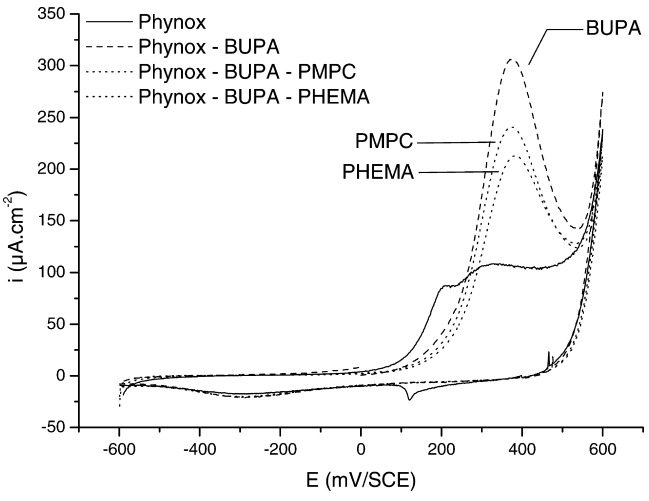

Figure 4. Cyclic voltammograms of a bare polished Phynox substrate, Phynox substrate modified with 11-(2-bromoisobutyrate)-undecyl-1-phosphonic acid (BUPA), modified Phynox substrate after ATRP polymerization of MPC or HEMA. (Curves acquired by scanning potentials from −600 mV/ECS to 600 mV/SCE at 20 mV·s^{-1} in NaOH 0.1 M).

BUPA does not significantly improve the corrosion resistance of Phynox substrates. Indeed, the corrosion current density and the corrosion potential values (Figure 3; Table 2) are similar for both bare Phynox and Phynox modified with BUPA

Table 2. Corrosion Current Density (i_{corr}) and Corrosion Potential (E_{corr}) of a Bare Polished Phynox Substrate, Phynox Substrate Modified with BUPA, Modified Phynox Substrates after ATRP (Co)polymerization of MPC, HEMA, HEMA-*b*-MPC, or HEMA-*s*-MPC (with Different Molar Ratios)

substrates	i_{corr} (10^{-7}A.cm^{-2})	E_{corr} (mV/SCE)
bare Phynox	1.22	−437
Phynox−BUPA	1.18	−410
Phynox − BUPA−PMPC	0.79	−400
Phynox−BUPA−PHEMA	0.71	−400
Phynox−BUPA−P(HEMA-*b*-MPC) 1/1	0.37	−295
Phynox−BUPA−P(HEMA-*b*-MPC) 2/1	0.39	−283
Phynox−BUPA−P(HEMA-*b*-MPC) 4/1	0.33	−297
Phynox−BUPA−P(HEMA-*s*-MPC) 1/1	0.53	−355
Phynox−BUPA−P(HEMA-*s*-MPC) 2/1	0.60	−356
Phynox−BUPA−P(HEMA-*s*-MPC) 4/1	0.43	−360

(around 10^{-7}A·cm^{-2} and −410 mV/SCE, respectively). However, cyclic voltammetry analyses (Figure 4) reveal an oxidation peak at 375 mV/SCE, which can be attributed to the degradation of the grafted BUPA layer. This is in line with the results of Devillers et al., who reported the grafting of *n*-dodecanoic and undecanoic phosphonic acid on Phynox.[1] They observed a similar behavior on the cyclic voltammetry curves and attributed this higher oxidation potential wave to a degradation of the organic layer rather than oxidation of the substrate. More recently, Kruszewki et al. also reported a similar behavior in the case of octadecylphosphonic acid and 16-phosphonohexadecanoic acid grafted on a cupronickel alloy.[31]

Nevertheless, these results establish and confirm that BUPA monolayers have been effectively and reproducibly grafted on the Phynox substrates in the applied modification conditions, in good correspondence with previously reported results.[19]

This is of importance considering the fact that BUPA grafting is a critical step for the surface initiated ATRP experiments to be achieved in this work.

3.2. ATRP Polymerization of MPC and HEMA on Phynox Substrates Modified with BUPA. First attempts of ATRP polymerization of MPC on Phynox have been published in a previous work.[19] In the present study, more comprehensive characterizations (linear sweep voltammetry and cyclic voltammetry) of the formed polymer layers have been used to provide a better insight on the characteristics of the formed polymer layers. ATRP polymerization of HEMA will also be presented and discussed.

After the ATRP polymerization of MPC and HEMA on Phynox substrates modified with BUPA, the substrates were first characterized by water static contact angle measurements (Table 1). The polymerization of MPC and HEMA in aqueous medium lead to a much more hydrophilic surface (32° and 35° respectively) than the bare Phynox substrate (52°) or the BUPA-modified Phynox substrate (87°). These results were expected given the hydrophilic nature of these polymers and are comparable with those previously reported in the literature either for PMPC layer[16,19,32−34] or PHEMA layer.[32,35,36]

The modified substrates were also characterized by XPS. Figure 2 shows representative survey spectra of a bare Phynox

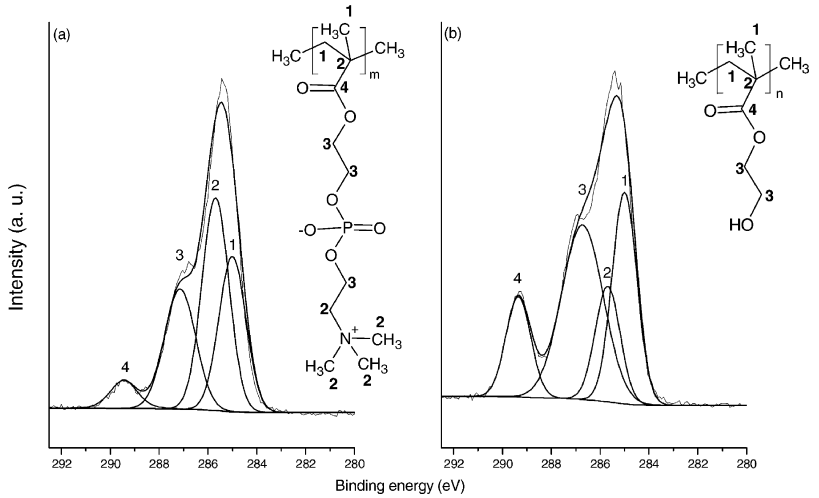

Figure 5. XPS C 1s core level spectra of a modified Phynox substrate after ATRP polymerization of MPC (a) or HEMA (b).

substrate, a Phynox substrate after the BUPA grafting and a modified Phynox after ATRP polymerization of MPC or HEMA. As expected the C 1s and O 1s core level peaks are more intense after the ATRP polymerization of MPC or HEMA. Moreover, most of the core level peaks attributed to the Phynox substrate (namely Ni 2p, Co 2p, Fe 2p, Mn 2p, and Mo 3d) are not visible anymore after ATRP polymerization of MPC or HEMA. The C 1s core level spectra (Figure 5) are analyzed with four components centered at a binding energy of 285.0 ($R-CH_3$), 285.7 ($R-CH_2-N^+-(CH_3)_3$, $R_3-C-COO-R$), 287.0 ($R-C-O-R$), and 289.4 eV ($R-C(O)O-R$) for both PMPC and PHEMA. These components are assigned to the various carbon species as illustrated in Figure 5 and are in good correspondence with the polymers chemical structures. The Br 3d core level peak is still present for both PMPC and PHEMA grafted Phynox substrates. It indicates that the polymerization process maintains the bromo-termination of the polymeric chains during their growth, which is in agreement with the ATRP mechanism.[8,9,37−40] It also evidence the living character of the polymerization and allows for further reinitiation and growth of a new polymeric structure. The main difference in the survey spectra of a modified Phynox substrate after ATRP polymerization of MPC and a modified Phynox substrate after ATRP polymerization of HEMA is the presence of the N 1s, P 2p, and P 2s core level peaks in the case of ATRP polymerization of MPC. Indeed, these atoms are constitutive of the MPC while they are not present in the HEMA structure. The calculated P/N ratio (where P and N are the normalized area of P 2p and N 1s components attributed to the phosphorus and nitrogen constitutive of the PMPC, respectively) is equal to 1.1, which agrees with the theoretical value (1.0). This suggests a good integrity in the structure of the formed PMPC layer. However, the analysis of the N 1s core level XPS spectrum of the HEMA covered surface (see the inset in Figure 2 d) reveals a weak nitrogen peak centered at 400.2 eV. This peak can be attributed to the nitrogen atoms present in PMDETA molecules that could have been entrapped in the polymer layer. This has also been observed in the case of ATRP polymerization of MPC in a previous study.[19]

According to the ellipsometry measurements (Table 1), it clearly appears that HEMA is polymerizing faster than MPC. Indeed for the same polymerization time and conditions, the PMPC layer is around 6.1 nm thick while PHEMA layer is around 23.1 nm. The density σ ($mol \cdot cm^{-2}$) of the grafted/polymerized monomers was calculated (Table 1) from ellipsometry thickness results for each grafted polymer using the equation: $\sigma = h\varphi/M$ where h is the ellipsometric thickness (nm), φ is the density of each dry polymer (1.30 $g \cdot cm^{-3}$ for PMPC and 1.15 $g \cdot cm^{-3}$ for PHEMA[32]), and M the molecular weight of the monomer (295.27 $g \cdot mol^{-1}$ for MPC and 130.14 $g \cdot mol^{-1}$ for HEMA). It appears that ATRP of the single components exhibits a HEMA density 7.5 times higher for HEMA than for MPC (2.0×10^{-8} and 2.7×10^{-9} $mol \cdot cm^{-2}$, respectively). Therefore, it appears that HEMA polymerizes about 7.5 times faster than MPC.

In order to characterize the impact of the formed polymer layers on the corrosion resistance of Phynox, the polarization curves of a bare Phynox substrate are compared with those of a Phynox substrate after the grafting of the initiator and a modified Phynox substrate after ATRP polymerization of MPC or HEMA (Figure 3; Table 2). It appears that the ATRP polymerization of MPC and HEMA on a modified Phynox substrate has a beneficial effect in term of corrosion resistance. The corrosion current density decreases from 1.2×10^{-7} $A \cdot cm^{-2}$ for a bare Phynox substrate down to 7.9×10^{-8} $A \cdot cm^{-2}$ and 7.1×10^{-8} $A \cdot cm^{-2}$ after ATRP polymerization of MPC and HEMA, respectively. In both cases the anodic current density has significantly decreased. Moreover, the corrosion potential is shifted toward more anodic values: from −437 mV/SCE for a bare Phynox substrate to −400 mV/SCE after ATRP polymerization of MPC and HEMA.

It can be noted that a PMPC layer is almost as protective as a PHEMA layer even with 7.5 times lesser graft density. It is thus anticipated that the protecting capacity of PMPC is intrinsically higher than PHEMA. It is likely due to the better coverage of the surface by PMPC. This is in agreement with the slower polymerization which allows the generation of shorter chains but from a larger number of anchoring sites (higher density of polymer chains). Increasing the thickness would be an interesting strategy in order to improve the protection of Phynox. This could be achieved by increasing the polymerization time, or by searching synergistic effect by combining thick hydrophilic layer of PHEMA and of PMPC in the generation of copolymer barriers.[40−44]

Cyclic voltammetry analyses (Figure 4), after ATRP polymerization of MPC and HEMA, reveal an attenuation of

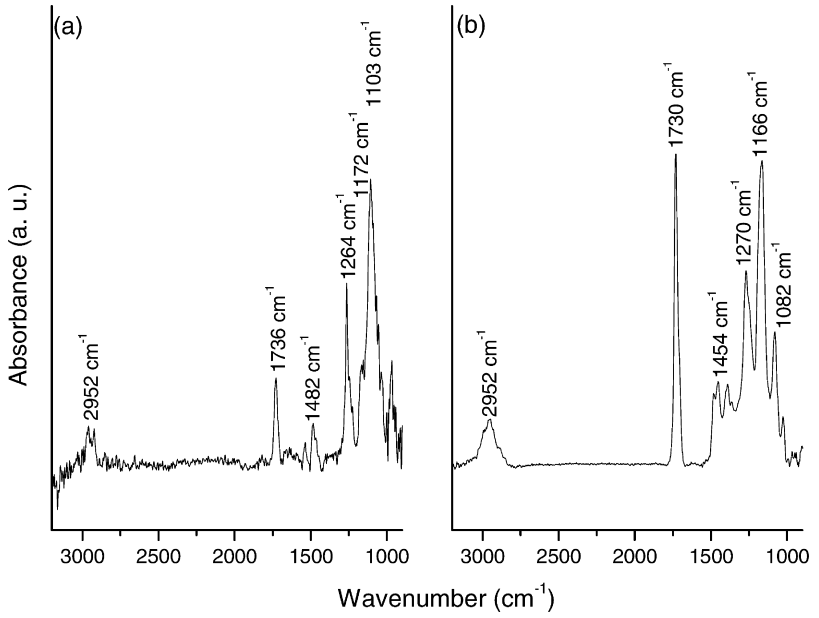

Figure 6. PM-IRRAS spectra of a modified Phynox substrate after ATRP polymerization of MPC (a) and after ATRP polymerization of HEMA (b).

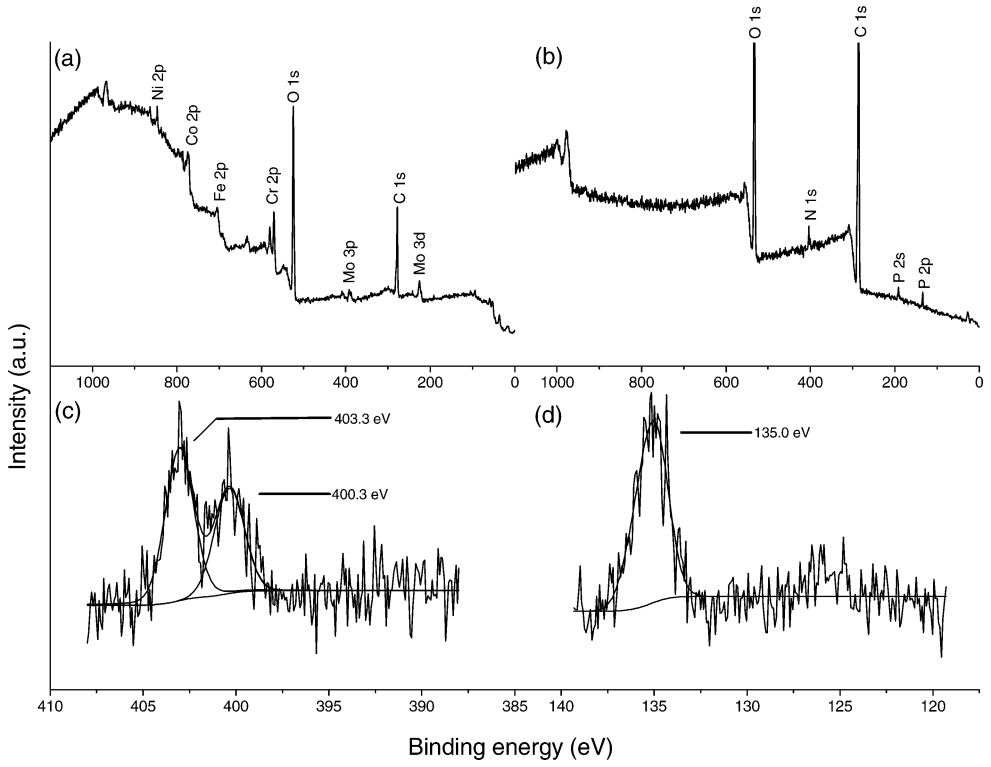

Figure 7. Representative XPS general survey spectra of bare polished Phynox substrate (a), a modified Phynox substrate after ATRP copolymerization of HEMA-*co*-MPC (b), N 1s (c), and P 2p (d) core levels spectra of a modified Phynox substrate after ATRP copolymerization of HEMA-*co*-MPC (block and statistic).

the oxidation peak attributed to the BUPA degradation at 375 mV/SCE. This attenuation is stronger after ATRP polymerization of HEMA compared to MPC. This can be explained by a better surface coverage as the PHEMA layer is thicker than the PMPC one. Ellipsometry measurements after cyclic voltammetry analyses reveal a slight decrease in thicknesses (from 6.1 to 5.1 nm for PMPC layer and from 23.1 to 21.2 nm for PHEMA layer). We can thus reasonably make the hypothesis that the oxidation process does not alter significantly the polymer chains. As this oxidation peaks have been previously attributed to the degradation of BUPA molecules, its attenuation after ATRP polymerization is likely due to the involvement of a significant proportion of these molecules into the polymerization process.

These substrates were also characterized by infrared spectroscopy. The spectra for a modified Phynox substrate after ATRP polymerization of MPC or HEMA is presented in Figure 6. The spectra reveals adsorptions bands in agreement

with the chemical structure of the polymers (the attributions are given in Supporting Information).

At this stage, we can conclude that the surface-initiated ATRP polymerization of MPC and HEMA on a modified Phynox has been carried out successfully and that the initiator ensures a robust link between the formed polymer layer and the Phynox substrate.

3.3. ATRP Copolymerization of HEMA and MPC (Block and Statistic) On Phynox Substrates Modified with BUPA. In this section, the feasibility of the copolymer P(HEMA-*co*-MPC), block and statistic, is considered, taking benefit from the living character of ATRP polymerization to grow multilayered polymeric system from the Phynox surface.

After the ATRP copolymerization of HEMA-*co*-MPC on Phynox substrates modified with BUPA, the substrates were characterized by water static contact angle measurements (Table 1). Surprisingly, the value obtained after the formation of the copolymer is higher (around 48°, regardless the molar ratios between the monomers and the process, that is, block or statistic) than the one obtained for PMPC or PHEMA individually covered Phynox surfaces (32° and 35°, respectively). This effect can be explained by the fact that the surface occupied by a PMPC chain is twice as large as the one occupied by a PHEMA chain.[29] For block copolymers, the growth of a PHEMA brush leads to a dense, homogeneous and hydrophilic film during the first step of the synthesis. However, during the second step, the organization of the PMPC blocks over PHEMA leads to exposition of the less hydrophilic HEMA and MPC lateral chains leading to a higher contact angle value. The same phenomenon is at play during the statistic polymerization as similar contact angle is obtained for statistic and block polymerization. The molecular organization of the external interface is very similar for both statistic and block polymers. For statistic copolymers, MPC monomers intercalate with HEMA ones. As a PMPC chain is larger than a PHEMA one, this induces a less dense and organized layer due to the steric hindrance of a PMPC chain.

Theses modified substrates were also characterized by XPS. Figure 7 shows representative survey spectra of a bare Phynox substrate, a Phynox substrate after ATRP copolymerization of HEMA-*co*-MPC, as well as the N 1s and P 2p core level spectra for a copolymer covered surface (as these spectrum are similar regardless the polymerization process and the molar ratios, only one spectra in shown in Figure 7 in order to make the reading easier). It appears that the C 1s and O 1s core level peaks are more intense after the ATRP copolymerization of HEMA-*co*-MPC. Furthermore, all the core level peaks attributed to the Phynox substrate (namely Ni 2p, Co 2p, Fe 2p, Mn 2p, and Mo 3d) including the Cr 2p are not visible anymore. The C 1s core level spectrum can be analyzed, with the same four components as previously described (see section 3.2) centered at a binding energy of 285.0 ($R-CH_3$), 285.8 ($R-CH_2-N^+-(CH_3)_3$; $R_3-C-COO-R$), 287.2 ($R-C-O-R$) and 289.5 eV ($R-C(O)-O-R$) (Figure 8). The N 1s core level spectrum can be analyzed with two components: a first peak centered at a binding energy of 403.3 eV corresponding to the nitrogen atom in the ammonium group in the MPC structure and a second one centered at 400.3 eV which can be attributed to the nitrogen of the PMDETA, which might be entrapped in the polymer layer. The P 2p core level spectrum shows only one peak centered at a binding energy of 135.0 eV. This corresponds to the phosphorus constitutive of the MPC. As nitrogen and phosphorus are only present in the MPC structure

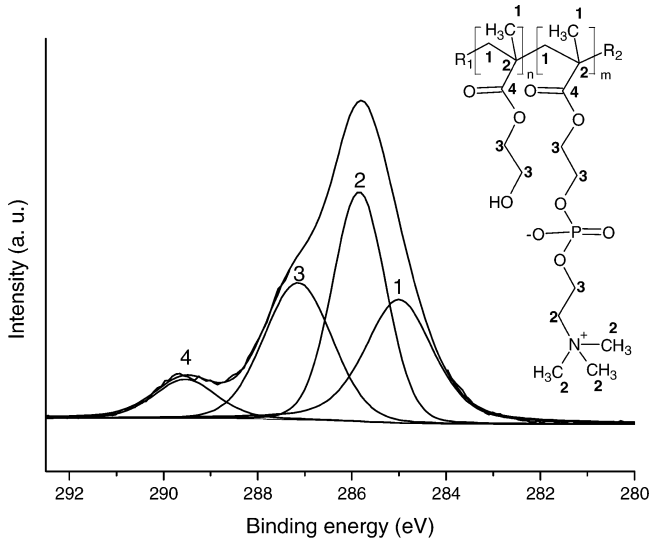

Figure 8. Representative XPS C 1s core level spectrum of a modified Phynox substrate after ATRP copolymerization of HEMA-*co*-MPC (block and statistic).

and not in the HEMA structure, it can be concluded that the block and statistic copolymerization did take place. The chemical integrity of the formed PMPC layers is assessed by the P/N calculated ratios presented in Table 1 (where P and N are the normalized area of P 2p and N 1s components attributed to the phosphorus and nitrogen constitutive of the PMPC, respectively). In each case, the experimental value is close to the theoretical value (1.0). In order to assess the proportion of each monomer in the different formed copolymer layers, N/C_{COOR} calculated ratios are also presented in Table 1 (where C_{COOR} is the normalized area of C 1s component attributed to the carbon of the ester function present in both PMPC and PHEMA structures). As the N 1s component is only present in the PMPC structure and the C $1s_{COOR}$ is present in both PMPC and PHEMA structures, we can assume that for m MPC and n HEMA monomer units in the formed copolymer layer, then the N 1s/C $1s_{COOR}$ ratio is equal to $m/(n + m)$. The n/m ratios are listed in Table 1. In block copolymerization process, a constant ratio close to 4.9 is obtained regardless the molar ratios used in the synthesis. This indicates a higher amount of HEMA than MPC and thus a thin PMPC layer formed on the PHEMA layer. In the statistic copolymerization process, these ratios are higher (about 13) compared to the block copolymerization process. Moreover, this ratio is increasing with a higher proportion of HEMA. These observations are in line with the fact that HEMA is polymerizing faster than MPC.

Ellipsometry measurements reveal similar thicknesses for block copolymerization (around 26 nm). This value is lower than the expected value of 29 nm (which is the sum of the thicknesses of the two polymers taken separately). However, termination reactions might happen during the ATRP process. Therefore, less propagation sites are available for the second step of the block copolymerization. This leads to a thinner PMPC layer (around 3 nm) than expected. This is in good correlation with the results obtained by XPS. For statistic copolymerization, ellipsometry measurements give a thickness around 28 nm. As this value is higher than a PHEMA layer, we can reasonably make the hypothesis that MPC chains, which

are larger than HEMA chains, are intercalating between the HEMA chains and swell the copolymer structure.

By combining the previous equation used for the grafting density σ calculation with the n/m ratios, σ of each monomer (σ_{MPC} and σ_{HEMA}) in these different copolymers layers (block and statistic) can be also determined (Table 1). For the block copolymer the σ_{MPC} value is obtained from the change in thickness between the PMPC and PHEMA polymerizations. In block copolymerization, σ calculated values are in line with previous observations and also reveal a lower value of σ_{MPC} (1.4×10^{-9} mol·cm^{-2}) compared to the PMPC homopolymer layer (2.7×10^{-9} mol·cm^{-2}) confirming a thinner PMPC layer after the block copolymerization. This yields to a ratio of HEMA and MPC monomers of the order of $\sigma_{HEMA}/\sigma_{MPC} \sim 14$ in the final block copolymers. This value is higher than that obtained by XPS as its analysis depth is restrained to the upper part of the polymer richer with the MPC block. The value of $\sigma_{HEMA}/\sigma_{MPC}$ is also twice higher than the value that could be obtained from comparison of the HEMA and MPC polymerization alone from BUPA modified Phynox surfaces. This means that a first polymerization step (HEMA polymerization) restrains the PMPC polymerization compared to a BUPA layer. This is attributed to the lower availability/density of polymerization sites from PHEMA than from the BUPA modified Phynox surfaces. It thus suggests that the density of PMPC chains grown from BUPA is twice higher than PMPC chains grown from PHEMA and confirms that MPC polymerization yields shorter and denser polymer chains than HEMA.

For statistic copolymerization, assuming that the polymer composition is homogeneous through the layer, the XPS n/m ratio corresponds to the $\sigma_{HEMA}/\sigma_{MPC}$ ratio. The respective values of σ_{HEMA} and σ_{MPC} are then given from the ellipsometry measurement. Regardless the molar ratio, similar σ_{HEMA} values are obtained (around 2.4×10^{-8} mol·cm^{-2}) which are close to a PHEMA homopolymer layer (2.0×10^{-8} mol·cm^{-2}). With an increasing amount of MPC, a slight increase of the σ_{MPC} is noticed (from 1.5×10^{-9} to 1.8×10^{-9} mol·cm^{-2}). The $\sigma_{HEMA}/\sigma_{MPC}$ value is again of the order of 13 as for block copolymerization. This confirms that the HEMA polymerization is the fastest process, which actually rules the initial density of grafted chains from the surface. This also agrees with the fact that σ_{HEMA} is not significantly different from that of pure PHEMA layers. The statistic polymer chains may then have the same density than those of PHEMA or of the block copolymers. The statistic coupling of MPC is too slow to alter significantly the polymer chain density. The statistic copolymerization allows, however, to disperse the MPC functionalities statistically within the polymer chains.

The reactivity ratios of each of the two monomers (r_{MPC} and r_{HEMA}) in the statistic copolymerization process has been evaluated by using the Mayo–Lewis equation (see Supporting Information). As different statistic copolymers have been synthesized with different molar ratios, the Fineman–Ross plot has been used to determine these reactivity ratios: $r_{MPC} = 0.65$ and $r_{HEMA} = 3.37$. As $r_{MPC} < 1$ and $r_{HEMA} > 1$, this indicates a random copolymer with HEMA units interacting mainly between them with occasional intercalations of MPC units. This is in good correlation with our previous observations; that is, HEMA is polymerizing faster than MPC.

The linear sweep voltammetry experiments (Figure 9; Table 2) show that the formation of copolymer has a synergistic effect in terms of corrosion resistance when compared to the results obtained for a PMPC or a PHEMA layer on a modified Phynox substrate. Indeed, regardless the copolymerization process, lower corrosion current densities (from 0.7×10^{-7} down to 0.3×10^{-7} A·cm^{-2}) and higher corrosion potentials (from −400 up to −283 mV/SCE) are obtained. Moreover, regardless the molar ratios, similar corrosion current densities and corrosion potentials are obtained either in the block copolymerization or in the statistic copolymerization process. Interestingly, the incorporation of a small fraction of MPC (<10%) moieties in PHEMA chains strongly impact the protection of the surface against corrosion. Moreover, it is not the only effect of MPC since polymerizing the same amount of MPC from the BUPA surface yields a layer much less protective than the copolymers. These results correspond to the sought synergistic effects. Owing to the large amount of HEMA monomer in the different layers, revealed by ellipsometry and XPS, the different PHEMA containing layers have a similar structure (similar density of grafted chains). The copolymerization process then completes this structure with the MPC moieties. This distribution is either statistic along the polymer chains or it is made from the top for the block copolymer layer.

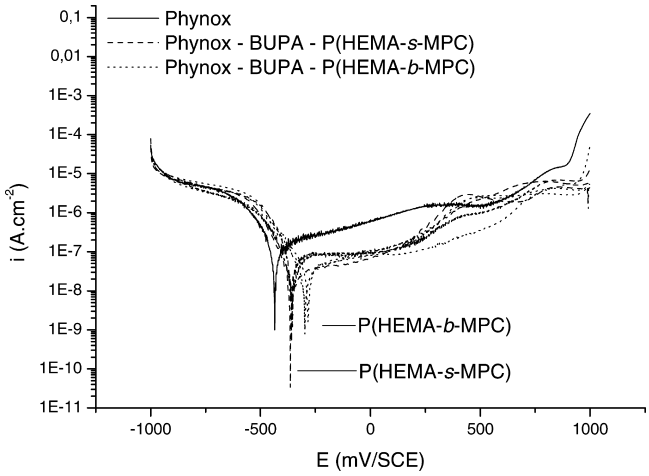

Figure 9. Linear sweep voltammetry curves of a bare polished Phynox substrate, modified Phynox substrates after ATRP copolymerization of HEMA-*co*-MPC (block and statistic). (Curves acquired by scanning potentials from −1 V/ECS to 1 V/SCE at 1 m·s^{-1} in NaCl 0.5 M).

Overall, slight differences are noticed between block copolymers and statistic copolymers. Block copolymers reveal slightly better effects in terms of corrosion resistance with slightly lower corrosion current densities and higher corrosion potentials (around 0.3×10^{-7} A·cm^{-2} and −290 mV/SCE) than statistic copolymers (around 0.5×10^{-7} A·cm^{-2} and −290 mV/SCE). This means that polymerizing PMPC from the top provides a more efficient barrier than the statistic inclusion of MPC features (statistically 1 MPC every 14 HEMA) within HEMA oligomers.

Cyclic voltammetry analyses (Figure 10) reveal an even stronger decrease of the oxidation peak attributed to the BUPA degradation compared to PMPC and PHEMA layers confirming the synergistic effect of the copolymerization. Regardless the copolymerization process and the molar ratios, similar oxidation peaks are obtained around 420 mV/SCE. Due to the fact that copolymer layers are thicker than PMPC and PHEMA layers (as previously demonstrated by ellipsometry), these thicker layers impart a better physical protection against the BUPA degradation. It is also interesting to notice (not shown in Figure 10), that even if the oxidations peaks are

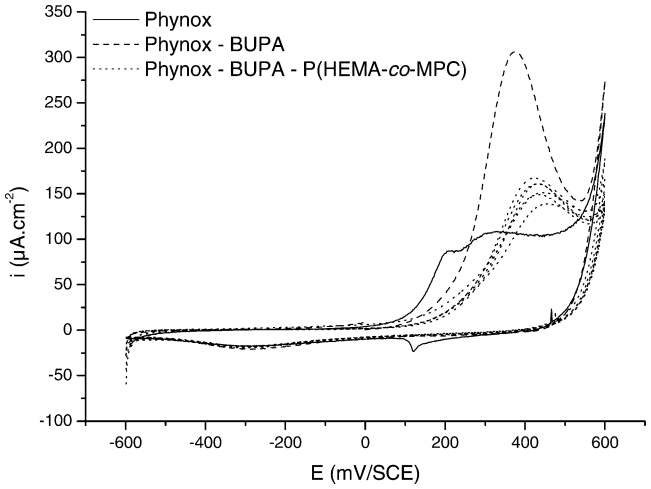

Figure 10. Cyclic voltammograms of a bare polished Phynox substrate, modified Phynox substrates after ATRP copolymerization of HEMA-*co*-MPC (block and statistic). (Curves acquired by scanning potentials from −600 mV/ECS to 600 mV/SCE at 20 mV·s^{-1} in NaOH 0.1 M).

similar, the peak intensity is always higher for statistic than for block copolymers. This reinforces the idea of a higher blocking of the access to free BUPA molecules from top filling PMPC chains than from statistic inclusion and thus an oxidation peak with lower current densities.

The PM-IRRAS spectrum for a modified Phynox substrate after ATRP copolymerization of HEMA-*co*-MPC is presented in Figure 11 (again, as all spectra obtained for block and statistic copolymerization with different molar ratios are similar, only one is presented in the figure for the sake of simplicity). The spectrum reveals adsorptions bands in agreement with the chemical structure of the copolymers (the attributions are given in Supporting Informations).

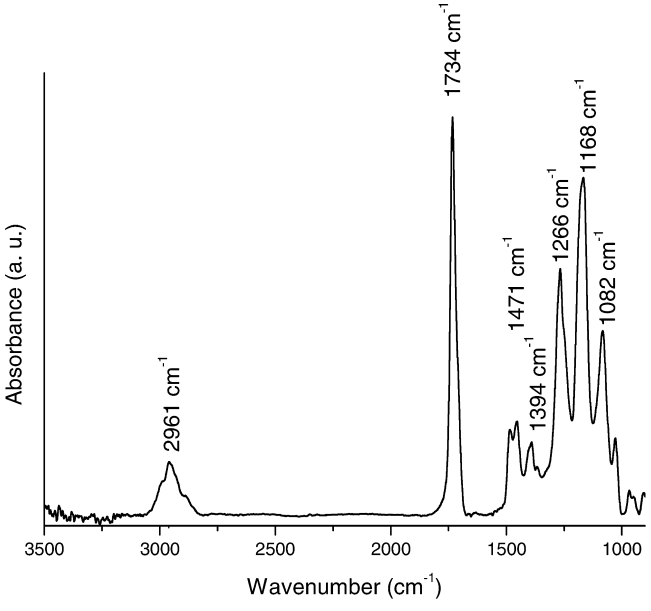

Figure 11. Representative PM-IRRAS spectrum of a modified Phynox substrate after ATRP copolymerization of HEMA-*co*-MPC (block and statistic).

4. CONCLUSIONS

The surface-initiated ATRP (co)polymerization of MPC and HEMA on Phynox substrates modified with 11-(2-bromoisobutyrate)-undecyl-1-phosphonic acid (BUPA) has been achieved.

First, the surface-initiated ATRP polymerization of MPC and HEMA has been successfully achieved on these modified Phynox substrates. The obtained polymer layers are hydrophilic and have a beneficial effect in term of corrosion resistance.

Second, the living character of ATRP polymerization allowed to grow either block or statistic copolymer P(HEMA-*co*-MPC) from Phynox surfaces. The obtained Phynox-BUPA-P(HEMA-*co*-MPC) surfaces are also hydrophilic but impart better properties in term of corrosion resistance than both individual layers. Spectroscopic and ellipsometric analyses reveal that all copolymers have the same density of grafted chains than the individual PHEMA layer. This is also true for the statistic copolymer as the MPC polymerization is much slower than the HEMA one. Introducing small fraction of PMPC in PHEMA (1 MPC for about 14 HEMA) provides a synergistic effect for the protection of the underlying Phynox surface. Even if block copolymers and statistic copolymers gave similar results in term of hydrophilicity, block copolymer appeared to be more efficient than statistic copolymers in term of corrosion resistance. This was explained by the more efficient filling of the PHEMA structure by PMPC chains than from statistic inclusion of MPC features along HEMA oligomers.

All these properties are essential parameters when developing systems designed to be applied in the biomedical devices field.

This works opens the prospect of copolymers brushes covalently attached to the substrate via the phosphonic acid anchoring group. Other copolymers and initiators will be investigated in future works with the prospect of a further increase of the corrosion resistance. The stability of the system in body simulation conditions should also be assessed. Induction heating instead of conventional heating might also be used for the triggering of ATRP.

■ ASSOCIATED CONTENT

Ⓢ Supporting Information

Optical models as well as the strategy used in the ellipsometry measurements. PM-IRRAS band attributions for the homopolymers and copolymers layers. Details about the Mayo−Lewis equation. This material is available free of charge via the Internet at http://pubs.acs.org/.

■ AUTHOR INFORMATION

Corresponding Author

*Tel: +32 81 72 52 30. Fax: +32 81 72 46 00. Email: zineb.mekhalif@unamur.be.

Notes

The authors declare no competing financial interest.

■ ACKNOWLEDGMENTS

The authors gratefully thank La Communauté Française de Belgique for financial support in the frame of "Concours des bourses de voyage−appel 2012".

■ REFERENCES

(1) Devillers, S.; Lanners, L.; Delhalle, J.; Mekhalif, Z. Grafting of Bifunctional Phosphonic and Carboxylic Acids on Phynox: Impact of Induction Heating. *Appl. Surf. Sci.* **2011**, *257*, 6252−6262.

(2) Es-Souni, M.; Fischer-Brandies, H.; Es-Souni, M. On the In Vitro Biocompatibility of Elgiloy, a Co-Based Alloy, Compared to Two Titanium Alloys. *J. Orofac. Orthop.* **2003**, *64*, 16−26.
(3) Clerc, C. O.; Jedwab, M. R.; Mayer, D. W.; Thompson, P. J.; Stinson, J. S. Assessment of Wrought ASTM F1058 Cobalt Alloy Properties for Permanent Surgical Implants. *J. Biomed. Mater. Res.* **1997**, *38*, 229−234.
(4) Sarikcioglu, L.; Demir, N.; Demirtop, A. A Standardized Method to Create Optic Nerve Crush: Yasargil Aneurysm Clip. *Exp. Eye Res.* **2007**, *84*, 373−377.
(5) De Beule, M.; Van Cauter, S.; Mortier, P.; Van Loo, D.; Van Impe, R.; Verdonck, P.; Verhegghe, B. Virtual Optimization of Self-Expandable Braided Wire Stents. *Med. Eng. Phys.* **2009**, *31*, 448−453.
(6) Halwani, D. O.; Anderson, P. G.; Brott, B. C.; Anayiotos, A. S.; Lemons, J. E. Clinical Device-Related Article Surface Characterization of Explanted Endovascular Stents: Evidence of In Vivo Corrosion. *J. Biomed. Mater. Res. B. Appl. Biomater.* **2010**, *95*, 225−238.
(7) Singh, R.; Dahotre, N. B. Corrosion Degradation and Prevention by Surface Modification of Biometallic Materials. *J. Mater. Sci. Mater. Med.* **2007**, *18*, 725−751.
(8) Siegwart, D. J.; Oh, J. K.; Matyjaszewski, K. ATRP in the Design of Functional Materials for Biomedical Applications. *Prog. Polym. Sci.* **2012**, *37*, 18−37.
(9) Barbey, R.; Lavanant, L.; Paripovic, D.; Schüwer, N.; Sugnaux, C.; Tugulu, S.; Klok, H. A. Polymer Brushes via Surface-Initiated Controlled Radical Polymerization: Synthesis, Characterization, Properties, and Applications. *Chem. Rev.* **2009**, *109*, 5437−5527.
(10) Aswal, D. K.; Lenfant, S.; Guerin, D.; Yakhmi, J. V.; Vuillaume, D. Self Assembled Monolayers on Silicon for Molecular Electronics. *Anal. Chim. Acta* **2006**, *568*, 84−108.
(11) Wasserman, S. R.; Tao, Y. T.; Whitesides, G. M. Structure and Reactivity of Alkylsiloxane Monolayers Formed by Reaction of Alkyltrichlorosilanes on Silicon Substrates. *Langmuir* **1989**, *5*, 1074−1087.
(12) Mutin, P. H.; Guerrero, G.; Vioux, A. Organic−Inorganic Hybrid Materials Based on Organophosphorus Coupling Molecules: From Metal Phosphonates to Surface Modification of Oxides. *Comptes Rendus Chim.* **2003**, *6*, 1153−1164.
(13) Marcinko, S.; Fadeev, A. Y. Hydrolytic Stability of Organic Monolayers Supported on TiO_2 and ZrO_2. *Langmuir* **2004**, *20*, 2270−2273.
(14) Raman, A.; Dubey, M.; Gouzman, I.; Gawalt, E. S. Formation of Self-Assembled Monolayers of Alkylphosphonic Acid on the Native Oxide Surface of SS316L. *Langmuir* **2006**, *22*, 6469−6472.
(15) Devillers, S.; Barthélémy, B.; Fery, I.; Delhalle, J.; Mekhalif, Z. Functionalization of Nitinol Surface toward a Versatile Platform for Post-grafting Chemical Reactions. *Electrochim. Acta* **2011**, *56*, 8129−8137.
(16) Devillers, S.; Barthélémy, B.; Delhalle, J.; Mekhalif, Z. Induction Heating vs Conventional Heating for the Hydrothermal Treatment of Nitinol and Its Subsequent 2-(Methacryloyloxy)ethyl 2-(trimethylammonio)ethyl Phosphate Coating by Surface-Initiated Atom Transfer Radical Polymerization. *ACS Appl. Mater. Interfaces* **2011**, *3*, 4059−4066.
(17) Quiñones, R.; Gawalt, E. S. Study of the Formation of Self-Assembled Monolayers on Nitinol. *Langmuir* **2007**, 10123−10130.
(18) Devillers, S.; Cuvelier, N.; Delhalle, J.; Mekhalif, Z. Grafting PEG Fragments on Phynox Substrates Modified with 11-Phosphoundecanoic Acid. *J. Electrochem. Soc.* **2009**, *156*, P177−P184.
(19) Barthélémy, B.; Devillers, S.; Minet, I.; Delhalle, J.; Mekhalif, Z. Surface-Initiated ATRP of 2-(Methacryloyloxy)ethyl 2-(trimethylammonio)ethyl Phosphate on Phynox. *Appl. Surf. Sci.* **2011**, *258*, 466−473.
(20) Babu, K.; Dhamodharan, R. Grafting of Poly(methyl Methacrylate) Brushes from Magnetite Nanoparticles Using a Phosphonic Acid Based Initiator by Ambient Temperature Atom Transfer Radical Polymerization (ATATRP). *Nanoscale Res. Lett.* **2008**, *3*, 109−117.
(21) Babu, K.; Dhamodharan, R. Synthesis of Polymer Grafted Magnetite Nanoparticle with the Highest Grafting Density via Controlled Radical Polymerization. *Nanoscale Res. Lett.* **2009**, *4*, 1090−1102.
(22) Kim, B. Y.; Ratcliff, E. L.; Armstrong, N. R.; Kowalewski, T.; Pyun, J. Ferrocene Functional Polymer Brushes on Indium Tin Oxide via Surface-Initiated Atom Transfer Radical Polymerization. *Langmuir* **2010**, *26*, 2083−2092.
(23) Minet, I.; Delhalle, J.; Hevesi, L.; Mekhalif, Z. Surface-Initiated ATRP of PMMA, PS, and Diblock PS-B-PMMA Copolymers from Stainless Steel Modified by 11-(2-Bromoisobutyrate)undecyl-1-Phosphonic Acid. *J. Colloid Interface Sci.* **2009**, *332*, 317−326.
(24) Ishihara, K.; Nomura, H.; Mihara, T.; Kurita, K.; Iwasaki, Y.; Nakabayashi, N. Why Do Phospholipid Polymers Reduce Protein Adsorption? *J. Biomed. Mater. Res.* **1998**, *39*, 323−330.
(25) Iwasaki, Y.; Ishihara, K. Cell Membrane-Inspired Phospholipid Polymers for Developing Medical Devices with Excellent Biointerfaces. *Sci. Technol. Adv. Mater.* **2012**, *13*, 1−14.
(26) Ye, S.; Jang, Y.; Yun, Y.; Shankarraman, V.; Woolley, J. R.; Hong, Y.; Gamble, L. J.; Ishihara, K.; Wagner, W. R. Surface Modfication of a Biodegradable Magnesium Alloy with Phosphorylcholine (PC) and Sulfobetaine (SB) Functional Macromolecules for Reduced Thrombogenicity and Acute Corrosion Resistance. *Langmuir* **2013**, *29*, 8320−8327.
(27) Kostina, N. Y.; Rodriguez-Emmenegger, C.; Houska, M.; Brynda, E.; Michálek, J. Non-fouling Hydrogels of 2-Hydroxyethyl Methacrylate and Zwitterionic Carboxybetaine (meth)acrylamides. *Biomacromolecules* **2012**, *13*, 4164−4170.
(28) Ishihara, K.; Oshida, H.; Endo, Y.; Ueda, T. Hemocompatibility of Human Whole Blood on Polymers with a Phospholipid Polar Group and Its Mechanism. *J. Biomed. Mater.* **1992**, *26*, 1543−1552.
(29) Inoue, Y.; Ishihara, K. Reduction of Protein Adsorption on Well-Characterized Polymer Brush Layers with Varying Chemical Structures. *Colloids Surf., B, Biointerfaces* **2010**, *81*, 350−357.
(30) Keller, R. N.; Wycoff, H. D. Copper(I) Chloride. *Inorg. Synth* **1946**, *2*, 1−4.
(31) Kruszewski, K. M.; Renk, E. R.; Gawalt, E. S. Self-Assembly of Organic Acid Molecules on the Metal Oxide Surface of a Cupronickel Alloy. *Thin Solid Films* **2012**, *520*, 4326−4331.
(32) Inoue, Y.; Nakanishi, T.; Ishihara, K. Adhesion Force of Proteins against Hydrophilic Polymer Brush Surfaces. *React. Funct. Polym.* **2011**, *71*, 350−355.
(33) Ishihara, K.; Goto, Y.; Takai, M.; Matsuno, R.; Inoue, Y.; Konno, T. Novel Polymer Biomaterials and Interfaces Inspired from Cell Membrane Functions. *Biochim. Biophys. Acta* **2011**, *1810*, 268−275.
(34) Feng, W.; Zhu, S.; Ishihara, K.; Brash, J. L. Protein Resistant Surfaces: Comparison of Acrylate Graft Polymers Bearing Oligo-Ethylene Oxide and Phosphorylcholine Side Chains. *Biointerphases* **2006**, *1*, 50−60.
(35) Chen, R.; Zhu, S.; Maclaughlin, S. Grafting Acrylic Polymers from Flat Nickel and Copper Surfaces by Surface-Initiated Atom Transfer Radical Polymerization. *Langmuir* **2008**, *24*, 6889−6896.
(36) Qian, T.; Li, Y.; Wu, Y.; Zheng, B.; Ma, H. Superhydrophobic Poly(dimethylsiloxane) via Surface-Initiated Polymerization with Ultralow Initiator Density. *Macromolecules* **2008**, *41*, 6641−6645.
(37) Lin, C. Y.; Coote, M. L.; Gennaro, A.; Matyjaszewski, K. Ab Initio Evaluation of the Thermodynamic and Electrochemical Properties of Alkyl Halides and Radicals and Polymerization. *J. Am. Chem. Soc.* **2008**, *130*, 12762−12774.
(38) Braunecker, W. A.; Tsarevsky, N. V.; Gennaro, A.; Matyjaszewski, K. Thermodynamic Components of the Atom Transfer Radical Polymerization Equilibrium: Quantifying Solvent Effects. *Macromolecules* **2009**, *42*, 6348−6360.
(39) Tang, W.; Kwak, Y.; Braunecker, W.; Tsarevsky, N. V.; Coote, M. L.; Matyjaszewski, K. Understanding Atom Transfer Radical Polymerization: Effect of Ligand and Initiator Structures on the Equilibrium Constants. *J. Am. Chem. Soc.* **2008**, *130*, 10702−10713.
(40) Olivier, A.; Meyer, F.; Raquez, J.-M.; Damman, P.; Dubois, P. Surface-Initiated Controlled Polymerization as a Convenient Method

for Designing Functional Polymer Brushes: From Self-Assembled Monolayers to Patterned Surfaces. *Prog. Polym. Sci.* **2012**, *37*, 157−181.
(41) Lu, G.; Li, Y.-M.; Lu, C.-H.; Xu, Z.-Z. Corrosion Protection of Iron Surface Modified by Poly(methyl Methacrylate) Using Surface-Initiated Atom Transfer Radical Polymerization (SI-ATRP). *Colloid Polym. Sci.* **2010**, *288*, 1445−1455.
(42) Yuan, S. J.; Pehkonen, S. O.; Ting, Y. P.; Neoh, K. G.; Kang, E. T. Inorganic−Organic Hybrid Coatings on Stainless Steel by Layer-by-Layer Deposition and Surface-Initiated Atom-Transfer-Radical Polymerization for Combating Biocorrosion. *ACS Appl. Mater. Interfaces* **2009**, *1*, 640−652.
(43) Liu, H.; Li, M.; Lu, Z.-Y.; Zhang, Z.-G.; Sun, C.-C. Influence of Surface-Initiated Polymerization Rate and Initiator Density on the Properties of Polymer Brushes. *Macromolecules* **2009**, *42*, 2863−2872.
(44) Jones, D. M.; Brown, A. A.; Huck, W. T. S.; Street, P.; Cb, C. Surface-Initiated Polymerizations in Aqueous Media: Effect of Initiator Density. *Langmuir* **2002**, *18*, 1265−1269.